Journal of Photochemistry & Photobiology, B: Biology 164 (2016) 43–48

Contents lists available at ScienceDirect

Journal of Photochemistry & Photobiology, B: Biology

journal homepage: www.elsevier.com/locate/jphotobiol

Photoinduced formation of thiols in human hair

M.V. Fedorkova [a], N.N. Brandt [b,*], A.Yu. Chikishev [b], N.V. Smolina [a], N.G. Balabushevich [c], S.A. Gusev [a], V.A. Lipatova [d], V.M. Botchey [e], G.E. Dobretsov [a], E.V. Mikhalchik [a]

[a] Federal Scientific Clinical Centre of Physical Chemical Medicine, Malaya Pyrogovskaya 1-a, Moscow 119435, Russia
[b] Faculty of Physics and International Laser Center, Lomonosov Moscow State University, Leninskiye Gory 1, bldg. 2, Moscow 119991, Russia
[c] Faculty of Chemistry, Lomonosov Moscow State University, Leninskiye Gory 1, bldg. 3, Moscow 119991, Russia
[d] Pirogov Russian National Research Medical University, Ostrovitianova 1, Moscow 117997, Russia
[e] Peoples' Friendship University of Russia, Miklukho-Maklaya 8, Moscow 117198, Russia

ARTICLE INFO

Article history:
Received 7 July 2016
Accepted 12 September 2016
Available online 13 September 2016

Keywords:
Photodegradation
Photodamage
Hair keratins
Disulfide bonds
Sulfhydryl groups
Thiols
Raman microspectroscopy

ABSTRACT

Raman, scanning electron, and optical microscopy of hair and spectrophotometry of soluble hair proteins are used to study the effect of UV-vis radiation on white hair. The samples of a healthy subject are irradiated using a mercury lamp and compared with non-irradiated (control) hair. The cuticle damage with partial exfoliation is revealed with the aid of SEM and optical microscopy of semifine sections. Gel filtration chromatography shows that the molecular weight of soluble proteins ranges from 5 to 7 kDa. Absorption spectroscopy proves an increase in amount of thiols in a heavier fraction of the soluble proteins of irradiated samples under study. Raman data indicate a decrease in the amount of S—S and C—S bonds in cystines and an increase in the amount of S—H bonds due to irradiation. Such changes are more pronounced in peripheral regions of hair. Conformational changes of hair keratins presumably related to the cleavage of disulfide bonds, follow from variations in amide I and low-frequency Raman bands. An increase in the content of thiols in proteins revealed by both photometric data on soluble proteins and Raman microspectroscopy of hair cuts can be used to develop a protocol of the analysis of photoinduced hair modification.

1. Introduction

Hair cortex predominantly consists of fibrillar insoluble proteins (keratins) and low-molecular-weight proteins (21 families with relatively high content of cystein) [1,2,3].

Photodamage of hair keratins under UV irradiation involves photodegradation of aromatic amino acids (tryptophan, tyrosine, and phenylalanine) and cystine [4,5]. Hair weathering caused by sunlight depends on UV-induced destruction of cystine [6,7].

UV absorption leads to the transition of amino acids to excited states, and further reactions depend on pH of solution, temperature, polarity of neighboring side chains, and protein structure [4,8]. In particular, thiyl radical that is formed due to photon absorption by disulfide bond or interaction of disulfide bond with triplet tyrosines or tryptophans may abstract hydrogen atom from alanine or glycine and can be reduced to thiol [9,10]. UVB-induced formation of thiols was registered after in vitro irradiation of epidermal growth factor [11], plasminogen [12], apo-α-lactalbumin [13], and insulin [14]. Oxidation of thiyl radical leads to formation of sulfonic and sulfinic acids [4,6,15]. Photons can be absorbed by disulfide bonds of both low-molecular-weight soluble proteins and fibrillar keratins of cortex. The results of [3,16,17,18] show that hair damage by bleaching reagents as well as UV radiation causes an increase in the amount of soluble proteins extracted from hair shaft in aqueous medium.

Raman spectroscopy is known to be helpful in the study of protein structure. In particular, conformations of disulfide bridges and the secondary structure of protein molecules can be analyzed. The measurements in the low-frequency range make it possible to characterize conformational changes of a protein molecule as a whole [19]. Raman microspectroscopy can be used to study effect of irradiation on keratins using the analysis of Raman bands assigned to S—S, C—S, and S—H bonds. The presence of melanin, the granules of which absorb laser radiation and fluoresce, impedes the application of Raman spectroscopy [20,21]. For cuticle of unpigmented hair, the intensities of Raman bands assigned to S—S and C—S bonds are higher than the corresponding intensities for cortex [20]. Thus, we study effect of mercury-lamp irradiation on white hair of a healthy patient under laboratory conditions.

Optical microscopy and SEM are conventional methods used to study the structure of hair shaft, in particular, the surface roughness, scale thinning and fusion [22]. Gel-chromatography is a helpful tool in the study of soluble keratins in spite of their low content in hair extracts [23].

The purpose of this work is to prove cleavage of disulfide bonds of hair keratins resulting in the formation of thiols based on the experimental study of hair cuts and soluble proteins of hair.

* Corresponding author.
E-mail address: brandt@physics.msu.ru (N.N. Brandt).

http://dx.doi.org/10.1016/j.jphotobiol.2016.09.021
1011-1344/

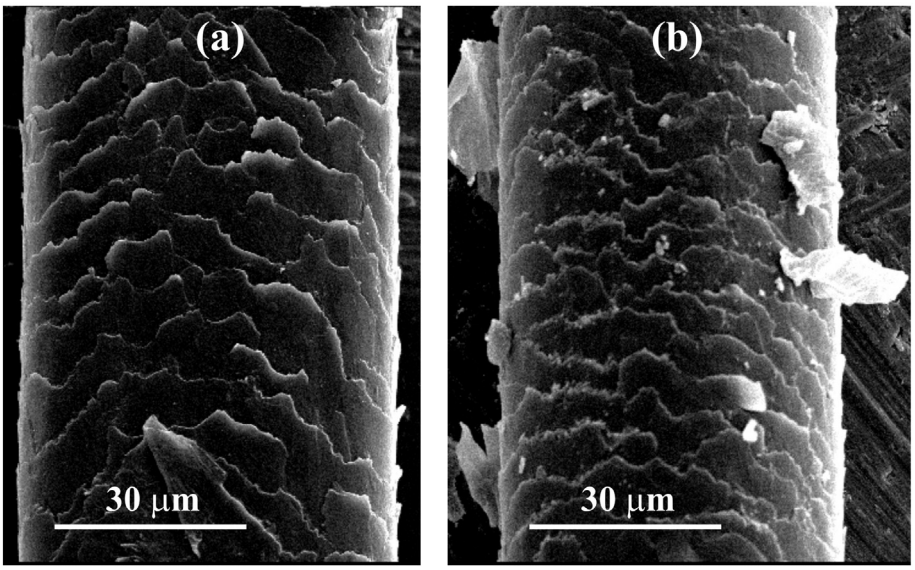

Fig. 1. SEM images of cuticle of (a) control and (b) irradiated hair shafts.

2. Materials and Methods

2.1. Samples

Unstained white (grey, unpigmented) hair from parietal region of a healthy patient were studied.

The following substances are used: Conducting Silver Paint (Ladd Research Industries); Romanovsky-Giemsa dye (Ecolab); araldite (Electron Microscopy Sciences); carbonate salts and Tris (Chimmed); PBS, DTNB (5,5′-dithio-bis(2-nitrobenzoic acid)), GSH (glutathione as a reduced form), bovine serum albumin (BSA), gel filtration molecular weight markers kit MW 12–200 kDa, soybean Bowman-Birk inhibitor, aprotinin from bovine lung, human insulin, and protamin from salmon (Sigma-Aldrich); and Total protein (Biuret) kit (Randox).

2.2. Irradiation

Hair samples are UV irradiated using a Medicor BLM-12 UV lamp. The spectrum of the lamp radiation is measured with the help of an Ocean Optics HR4000CG-UV-NIR spectrometer. The main emission bands of the lamp are picked at 254 (0.38), 366 (0.04), 406 (0.13), 437 (0.75), 547 (1), 578 (0.13), and 580 nm (0.13) (relative intensities of the bands are indicated in parentheses). The hair samples are placed at a distance of 15 cm from the lamp, where the intensity at a wavelength of 254 nm is about 30 μW/cm^2. (Note that the published results on the total sunlight intensity in the UVB region are 78 μW/cm^2 (280–315 nm) [24], 40 μW/cm^2 in December (below 313 nm) [25], and 175 μW/cm^2 in summer (below 313 nm) [25].) Radiation intensities are measured with the aid of a Coherent FieldMaster FM powermeter. Irradiation time is 6 h, so that the total energy density is 4.4 J/cm^2 and the energy density at a wavelength of 254 nm is 0.65 J/cm^2.

2.3. Scanning Electron and Optical Microscopy

A Hitachi S-570 scanning electron microscope is used for SEM measurements. The samples are placed on a sample stage and fixed using a Ladd Research Industries Conducting Silver Paint. The samples are covered with a 10-nm-thick layer of Pt-Pd alloy in an Eiko IB-3 Ion Coater.

For optical microscopy samples are processed using a conventional method for electron microscopy study with subsequent imbedding in araldite [26]. Semifine sections are obtained using a Reichert-Jung Ultracut ultramicrotome and stained with the aid of the Romanowsky-Giemsa procedure for histological analysis. A Nikon Eclipse E200 microscope with a DS-Fi1 camera head is employed.

2.4. Eluted and Soluble Hair Proteins

For the quantification of eluted proteins, 1–5 mg of hair fragments with a length of about 1 cm are incubated in 1 mL of 0.1 M carbonate buffer solution (pH 10.5) over 30 min in a shaker at room temperature. Then, the eluate is centrifuged at 900*g* over 20 min. Protein concentration is estimated using optical absorption at a wavelength of 240 nm

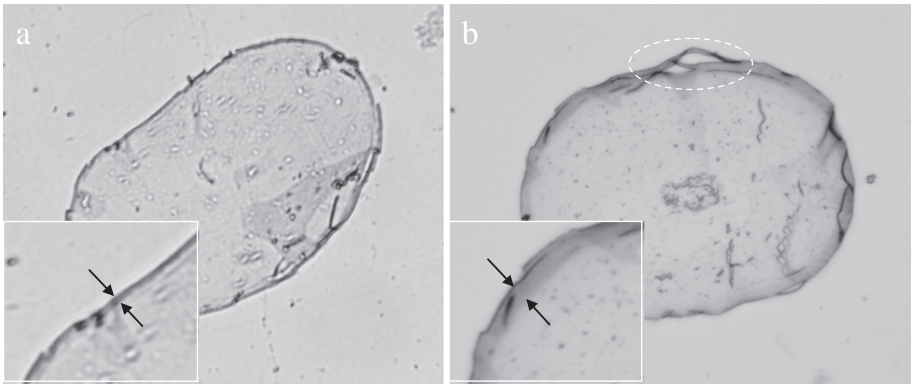

Fig. 2. Cuts of (a) control and (b) irradiated hair. The arrows show the estimated thickness of highly stained layers. The dashed line shows the fragment with exfoliated cuticle.

Table 1
Effect of UV irradiation on soluble proteins in hair shaft.

Samples	Protein content, μg/mg	Thiol (SH) content, μg/(g of protein)
Control	265 ± 64	0,9 ± 0,2
Irradiated	272 ± 59	2,1 ± 0,4

(Shimadzu 1700UV spectrophotometer). BSA solution is used for calibration. Finally, the mass of eluted proteins per unit mass of hair is calculated.

For the study of soluble compounds, hair (2–5 mg) are homogenized in a glass Potter homogenizer to obtain suspension in 1 mL of 0.1 M carbonate buffer solution (pH 10.5). The suspension is centrifuged over 30 min at 900*g*. The concentration of proteins in supernatant is estimated using optical absorption at a wavelength of 240 nm. Finally, the mass of soluble proteins per unit mass of hair is calculated. To determine concentration of S-H groups (thiols), we add an aliquot of soluble proteins (350 μL) to 0.4 M tris buffer (pH 8.9, 650 μL), introduce DTNB to a concentration of 6.25 mM, and measure absorbance at 412 nm. Reduced glutathione (GSH) serves as reference substance. Relative content of SH groups is normalized by mass of protein.

2.5. Gel-Chromatography

Gel-chromatography is performed with the aid of a Knauer Smartline chromatograph with a Biofox 17 SEC (8 × 300 mm, BioWorks) column (0.2 mL of the sample solution is applied to the column). Elution is performed using PBS at a flow rate of 0.5 mL/min under monitoring of absorbance at a wavelength of 240 nm. The collection time for a single fraction is 1 min. The column is preliminary calibrated using gel filtration molecular weight markers kit MW 12–200 kDa (β-amilase from sweet potato (MW 200 kDa), alcohol dehydrogenase from yeast (MW 150 kDa), albumin from bovine serum (MW 66 kDa), carbonic anhydrase from bovine erythrocytes (MW 29 kDa), cytochrome *C* from horse heart (MW 12.4 kDa)), Bowman-Birk inhibitor (MW 8 kDa), aprotinin (MW 6.5 kDa), human insulin (MW 5.8 kDa), and protamin (MW 5 kDa).

2.6. Raman Microspectroscopy

Transverse hair cuts are studied with the aid of Thermo Scientific DXR Raman Microscope at an excitation wavelength of 780 nm and a laser power of 24 mW using a 50× objective. The measurements are performed at four points at a diameter of a hair cut in its peripheral and central regions (PRs and CRs, respectively) for 5-mm-long fragments from the central parts of 20-cm-long hair shafts. Backgrounds are subtracted using procedures of [27,28].

3. Results

3.1. Scanning Electron and Optical Microscopy

The results of [18] show that UV irradiation leads to an increase in the amount of eluted proteins by a factor of 1.5 possibly due to damage of cuticle and variations in its permeability. Indeed, SEM shows that the lamp irradiation causes an increase in surface roughness (Fig. 1), and we clearly observe scalloped edges of flakes and exfoliation of cuticle.

Optical microscopy of semifine stained sections (Fig. 2) shows an increase in the thickness of external layer containing dye. On average, the thickness of the stained layer in irradiated samples is greater than the thickness of such a layer in control samples by a factor of 2.

Fig. 2b also shows exfoliation of cuticle for irradiated hair. The zone of stained upper cortex layer is clearly seen under the exfoliated cuticle.

3.2. Analysis of Soluble Proteins

Absorption measurements show that UV irradiation does not affect the content of soluble proteins in hair shaft (Table 1). However, the concentration of thiols in soluble proteins of irradiated hair noticeably increases.

Gel filtration chromatography (Fig. 3) is used to study solutions containing soluble proteins, which give positive result to the biuret test. The inset shows the results of calibration using several proteins with different molecular weights and chromatographic data. We observe two peaks of soluble proteins with molecular weights in an interval of 5–7 kDa. Note redistribution of peak intensities due to irradiation.

Ellman's reagent (DTNB solution) is added to 0.5 mL chromatographic fractions in a time interval of 16–33 min to estimate the concentration of thiols in soluble proteins. The results are in agreement with the above photometric data and yield an increase in thiol content by a factor of about 2 for fraction collected in an interval of 24–27 min for irradiated samples.

3.3. Raman Measurements of Hair Cuts

Fig. 4 shows averaged Raman spectra of PRs prior to and after UV irradiation and CRs after irradiation. We do not present Raman spectrum of CR prior to irradiation, since it is identical to the corresponding PR

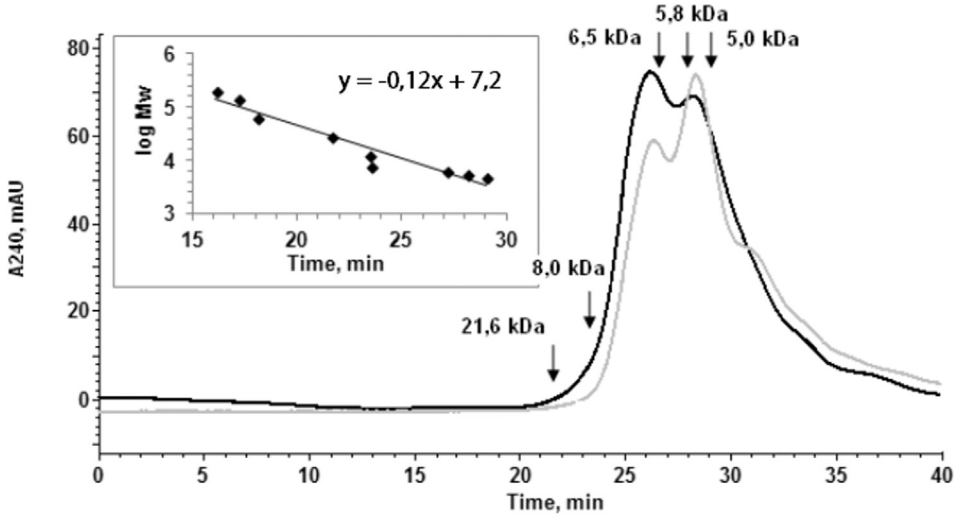

Fig. 3. Chromatograms of soluble proteins of (black line) irradiated and (grey line) control hair. The inset shows results of calibration using several proteins with known molecular weights. The arrows show the positions of peaks corresponding to reference proteins.

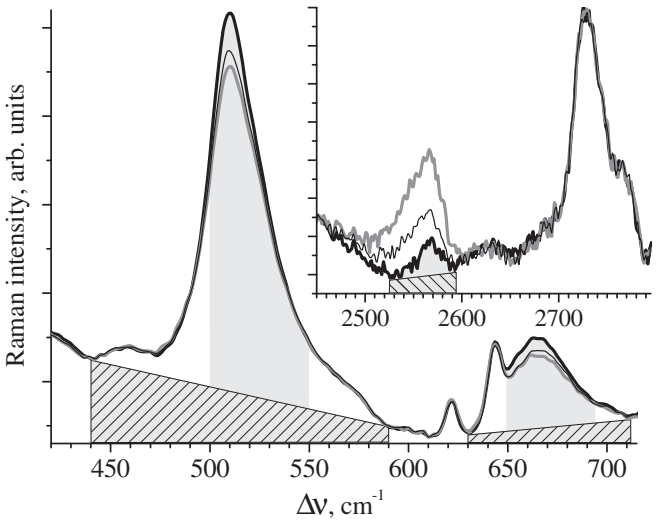

Fig. 4. Averaged Raman spectra of hair cuts measured in PRs of (thick black line) control and (thick grey line) irradiated samples and (thin black line) CRs of irradiated sample.

spectrum. Linear backgrounds (hatched areas) are subtracted in each spectral interval under study (440–590 cm^{-1} (S—S), 630–712 cm^{-1} (C—S), and 2501–2598 cm^{-1} (S—H)). Then, integral intensities are calculated in spectral intervals of 500–550 cm^{-1} (S—S), 649–694 cm^{-1} (C—S), and 2525–2594 cm^{-1} (S—H) (shaded areas).

Fig. 5 presents resulting averaged integral intensities with standard errors for PRs and CRs prior to and after UV irradiation. For comparison, integral intensity in each spectral interval is normalized by the integral intensity of PR prior to UV irradiation in the same interval. Sulfhydryl groups (S—H) are uniformly distributed over cross section of control hair. Most developed spectral changes caused by UV irradiation are observed for PRs. The content of S—S and C—S bonds of cystines decreases and the amount of S—H bonds substantially increases. Apparently, cleavage of disulfide bridges takes place in PRs and relative content of cysteine residues consequently increases. The same tendencies are observed for CRs after irradiation but the changes are substantially weaker.

It is known that disulfide bonds stabilize protein structure. Therefore, the cleavage of such bonds may lead to the changes in the structure of protein molecule as a whole (in particular, secondary structure) and rigidity and shape of the molecule. Thus, to additionally prove the cleavage of disulfide bonds, we analyze (i) the low-frequency range of Raman spectra, the bands of which can be assigned to skeletal and side chain vibrations and collective motions of atomic groups in a protein molecule [20,29] and (ii) the Amide I band, which can be used to characterize the secondary structure [30,31].

Low-frequency Raman spectra of CRs and PRs prior to and after irradiation are generally similar to each other. To reveal the spectral differences, we calculate second derivatives of the spectral curves. Three second-derivative curves (CRs prior to and after irradiation and PR prior to irradiation) almost coincide with each other and exhibit a broad band peaked at 153 cm^{-1}. UV irradiation gives rise to an intense Raman band peaked at 147 cm^{-1} in the spectrum of PR (Fig. 6). It is seen that intensity variations in the low-frequency spectral range are comparable with variations in the spectral interval of disulfide bonds.

The second derivatives of spectral curves also allow a more detailed analysis of variations in the intensities of Raman bands assigned to disulfide bonds. It is seen that a decrease in the Raman intensity at 510 cm^{-1} by approximately 30% (S—S stretching vibrations in the gauche-gauche-gauche (ggg) conformation) is accompanied by an increase in the intensities at 525 and 545 cm^{-1} (trans-gauche-gauche (tgg) and trans-gauche-trans (tgt) conformations, respectively). This circumstance indicates that the cleavage of disulfide bonds is accompanied by transformations of ggg disulfide bridges in keratins into tgg and tgt bridges.

Fig. 7 presents amide I bands in averaged Raman spectra of hair cuts. The spectra are normalized by integral intensities in the spectral interval of 1630–1750 cm^{-1}. The second derivatives of spectral curves (Fig. 7b) clearly show three main components at 1654, 1672, and ~1692 cm^{-1}. In accordance with the results of [32], the components can be assigned to α-helices, β-sheets, and random coil and β-turns, respectively. It is seen that UV irradiation causes minor changes in the secondary structure of hair proteins.

4. Discussion

It is known that the photooxidation of cystine is caused by both UV and visible radiation. The UV radiation is more efficient [7,15], since molar absorption coefficients of cystine are 270 M^{-1} cm^{-1} at 254 nm [33] and 70 M^{-1} cm^{-1} at 288 nm [34]. Thus, BLM-12 UV can be used in the experiments on photodegradation of cystine in human hair although the lamp radiation poorly imitates solar radiation.

The experimental results can be used to develop protocol of the analysis of hair degradation under UV and visible (including solar) irradiation. The content of thiols in soluble proteins may serve as a marker in such analysis. Moreover, as it was shown by Hoting et al. [15], IR radiation also influences cystine content in human hair, and this finding also needs further investigation.

SEM and optical microscopy images show typical signs of photoinduced cuticle damage (focal losses of cuticular edges and cuticular detachments), which are in agreement with the results of [35]. Such photodamage may facilitate leakage of soluble keratins from hair shaft into water which is registered as an increase in the amount of eluted proteins, that was also shown in [16,36].

The observed increase in the thickness of the stained layer in irradiated hair (Section 3.1) is due to the fact that methylene blue, contained in the Romanowsky-Giemsa dye, binds with acidic products of the destruction of disulfide bonds in keratins [37].

Gel-electrophoresis, isoelectric focusing, and gel filtration chromatography of keratins extracted from human hair yield the presence of

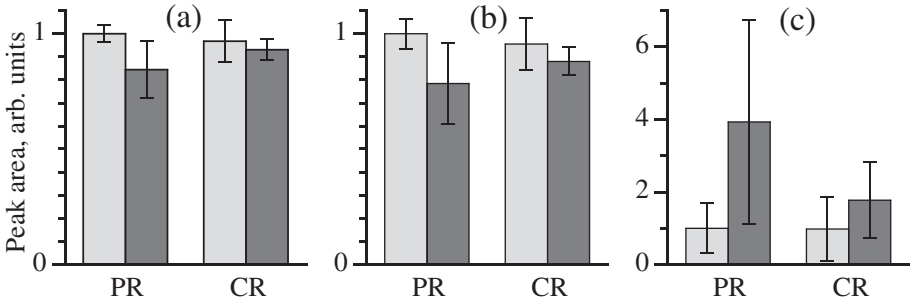

Fig. 5. Integral Raman intensities of PRs and CRs for spectral intervals of (a) 500–550 (S—S), (b) 649–694 (C—S), and (c) 2525–2594 (S—H) cm^{-1} of (grey columns) control and (black columns) irradiated samples (see text for details).

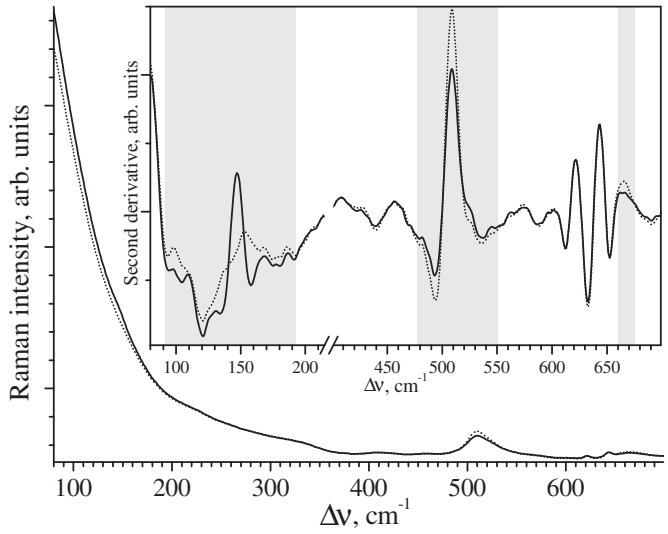

Fig. 6. Averaged Raman spectra of PRs of control (dotted line) and irradiated (solid line) samples. The inset shows the corresponding second derivatives.

polypeptides with MWs of 16 and 12 kDa with pI 7.4–5.4 [23]. In our experiments, an increase in the content of soluble proteins with an MW of 6–7 kDa can be due to the cleavage of intermolecular disulfide bonds and/or damage of high-molecular keratins with formation of soluble fragments. This could be another reason for an increase in the amount of proteins extractable from hair shaft (eluted proteins) [17].

Normally, low-frequency Raman bands in spectra of proteins are assigned to backbone vibrations, torsional vibrations of side groups, and intermolecular vibrations. Thus, we may assume general conformational changes of keratins in PRs due to the cleavage of disulfide bonds in irradiated hair. Minor changes in the secondary structure of proteins in irradiated hair follow from variations in relative intensities of spectral components of amide I band. Photoinduced damage of indole ring in tryptophan and oxidation to kynurenine [8] may also significantly change conformation of protein as was shown for various crystallins [38]. Earlier, we have shown a decrease in tryptophan autofluorescence in soluble keratins from human hair after UV-irradiation [18]. Thus, the changes in the secondary structure of hair proteins can be caused by both damage of disulfide bonds and tryptophan oxidation. Although, the UV-induced changes in signals of the secondary-structure elements

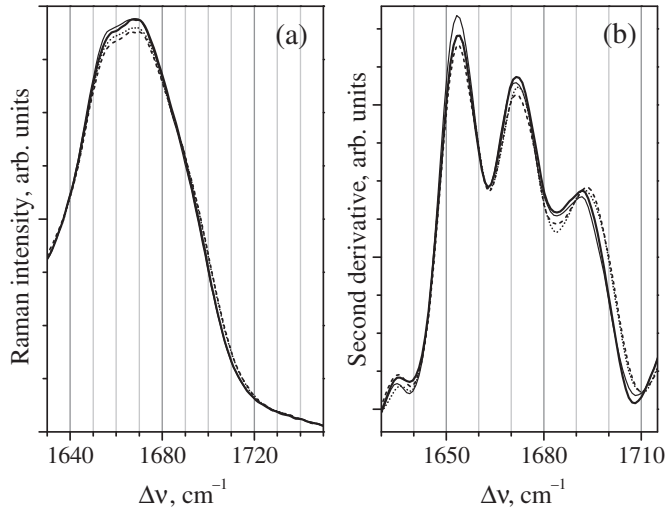

Fig. 7. (a) Averaged Raman spectra of PRs (dashed and thick solid lines) and CRs (dotted and thin solid lines) of control (solid lines) and irradiated samples(dashed and dotted lines) and (b) the corresponding second derivatives.

are within several percents, we may assume that the effect depends on the irradiation doze.

The fact that the chromatographic results are in agreement with Raman data indicates that the formation of S—H bonds is, at least, partially related to the cleavage of disulfide bonds rather than chemical reactions that are used to obtain fraction of soluble proteins, since the Raman data are obtained for chemically untreated hair.

5. Conclusion

UV irradiation causes damage of cuticle and an increase in the amount of SH groups in proteins of hair shaft (including an increase in soluble proteins of hair). The amount of S—S and C—S bonds of cystines decreases and such an effect is more developed for peripheral regions. Conformational changes of hair keratins presumably related to the cleavage of disulfide bonds, follow from variations in amide I and low-frequency Raman bands. Gel filtration chromatography shows that the molecular weight of soluble proteins ranges from 5 to 7 kDa.

Both photometric data on soluble proteins and Raman microspectroscopy of hair cuts indicate an increase in the content of thiols in proteins. This result can be helpful for development of a protocol of the analysis of hair modification under UV, visible, and IR irradiation.

Acknowledgments

DXR Raman microscope was purchased with the help of the Program of Development, Moscow State University.

References

[1] L.J. Sundström, Wolfram, human hair: a unique physicochemical composite, J. Am. Acad. Dermatol. 48 (2003) 106–114.
[2] A.C. Nogueira, A.K. Nakano, I. Joekes, Impairment of hair mechanical properties by sun exposure and bleaching treatments, J. Cosmet. Sci. 55 (2004) 533–537.
[3] E. Fernandez, C. Barba, C. Alonso, M. Marti, J.L. Parra, L. Coderch, Photodamage determination of human hair, J. Photochem. Photobiol. B 106 (2012) 101–106.
[4] B.A. Kerwin, R.L. Remmele Jr., Protect from light photodegradation and protein biologics, J. Pharm. Sci. 96 (2007) 1468–1479.
[5] S.A. Hibbert, R.E.B. Watson, N.K. Gibbs, P. Costello, C. Baldock, A.S. Weiss, C.E.M. Griffiths, M.J. Sherratt, A potential role for endogenous proteins as sacrificial sunscreens and antioxidants in human tissues, Redox Biol. 5 (2015) 102–113.
[6] K.R. Millington, J.S. Church, The photodegragation of wool keratin. II. Proposed mechanisms involving cystine, J. Photochem. Photobiol. B 39 (1997) 204–212.
[7] V. Signori, Review of the current understanding of the effect of ultraviolet and visible radiation on hair structure and options for photochemistry, J. Cosmet. Sci. 55 (2004) 95–113.
[8] M.T. Neves Petersen, S. Klitgaard, E. Skovsen, T. Pascher, T. Polivka, S.B. Petersen, A. Yartsev, V.I. Sundström, Flash photolysis of cutinase: identification and decay kinetics of transient intermediates formed upon UV excitation of aromatic residues, Biophys. J. 97 (2009) 211–226.
[9] R. Zhao, J. Lind, G. Merenyl, T.E. Eriksen, Kinetics of one-electron oxidation of thiols and hydrogen abstraction by thyil radicals from α-amino C-H bonds, J. Am. Chem. Soc. 116 (1994) 12010–12015.
[10] O. Mozziconacci, V. Sharov, T.D. Williams, B.A. Kerwin, C. Schöneich, Peptide cyteine thiyl radicals abstract hydrogen atoms from surrounding amino acids: the photolysis of a cystine containing model peptide, J.Phys.Chem. B 112 (2008) 9250–9257.
[11] M. Correia, T. Viruthachalam, I. Coutinho, G.G. Prakash, S.B. Petersen, M.T. Neves-Petersen, Modulating the structure of EGFR with UV light: new possibilities in cancer therapy, PLoS One 9 (2014), e111617.
[12] M. Correia, M.T. Neves-Petersen, T. Snabe, T. Viruthachalam, S.R.R. Campos, A.M. Baptista, S.B. Petersen, Photonic activation of plasminogen induced by low dose UVB, PLoS One 10 (2015), e0116737.
[13] M. Correia, M.T. Neves-Petersen, A. Parracino, A. Kold, S.B. Petersen, Photophysics, photochemistry and energetics of UV light induced disulphide bridge disruption in apo-α-lactalbumin, J. Fluoresc. 22 (2012) 323–337.
[14] M. Correia, M.T. Neves-Petersen, P.B. Jeppesen, S. Gregersen, S.B. Petersen, UV-light exposure of insulin: pharmaceutical implications upon covalent insulin dityrosine dimerization and disulphide bond photolysis, PLoS One 7 (2012), e50733.
[15] E. Hoting, M. Zimmermann, S. Hilterhaus-Bong, Photochemical alterations in human hair. I. Artificial irradiation and investigations of hair proteins, J. Soc. Cosmet. Chem. 46 (1995) 85–99.
[16] S.S. Sandhu, C.R. Robbins, A simple and sensitive technique, based on protein loss measurements, to assess surface damage to human hair, J. Soc. Cosmet. Chem. 44 (1993) 163–175.
[17] T. Inoue, M. Ito, K. Kizawa, Labile proteins accumulated in damage hair upon permanent waving and bleaching treatments, J. Cosmet. Sci. 53 (2002) 337–344.

[18] M.V. Fedorkova, N.V. Smolina, E.V. Mikhalchik, N.G. Balabushevich, G.A. Ibragimova, A.G. Gadzhigoroeva, E.I. Dmitrieva, G.E. Dobretsov, Effects of ultraviolet radiation on the soluble proteins of human hair, J. Photochem. Photobiol. B 140 (2014) 390–395.
[19] P.C. Painter, L.E. Mosher, C. Rhoads, Low-frequency modes in the Raman spectra of proteins, Biopolymers 21 (1982) 1469–1472.
[20] A. Kuzuhara, Analysis of structural change in keratin fibers resulting from chemical treatments using Raman spectroscopy, Biopolymers 77 (2005) 335–344.
[21] G. Zhang, L. Senak, D.J. Moore, Measuring changes in chemistry, composition, and molecular structure within hair fibers by infrared and Raman spectroscopic imaging, J. Biomed. Opt. 16 (2011) 056009.
[22] S. Ruetsch, Y. Kamath, H.-D. Weigmann, Photodegradation of human hair: an SEM study, J. Cosmet. Sci. 51 (2000) 103–125.
[23] M. Folin, E. Contiero, Electrophoretic analysis of human hair keratins, Anthropol. Anz. 53 (1995) 337–348.
[24] ASTM Subcommittee G03.09, ASTM G173-03 Standard Tables for Reference Solar Spectral Irradiance Direct Normal and Hemispherical on 37° Tilted Surface. Annual Book of ASTM Standards, Vol. 14.04, ASTM International, West Conshohocken, PA, 2003.
[25] A. Pirie, Formation of N′-formylkynurenine in proteins from lens and other sources by exposure to sunlight, Biochem. J. 125 (1971) 203–208.
[26] A.M. Glauert, Fixation, Dehydration and Embedding of Biological Specimens, Elsevier, Amsterdam, 1975 207.
[27] N.N. Brandt, A.Yu. Chikishev, A method of comparing Raman spectra, Laser Phys. 14 (2004) 1386–1392.
[28] N.N. Brandt, O.O. Brovko, A.Y. Chikishev, O.D. Paraschuk, Optimization of the rolling-circle filter for Raman background subtraction, Appl. Spectrosc. 60 (2006) 288–293.
[29] S.E. May Colaianni, O. Faurskov Nielsen, Low-frequency Raman spectroscopy, J. Mol. Struct. 347 (1995) 267–284.
[30] R.W. Williams, Estimation of protein secondary structure from the laser Raman amide I spectrum, J. Mol. Biol. 166 (1983) 581–603.
[31] R.W. Williams, A.K. Dunker, Determination of the secondary structure of proteins from the amide I band of the laser Raman spectrum, J. Mol. Biol. 152 (1981) 783–813.
[32] K.R. Ackermann, J. Koster, S. Schlucker, Polarized Raman microspectroscopy on intact human hair, J. Biophoton. 1 (2008) 419–424.
[33] A.D. McLaren, D. Shugar, Photochemistry of Proteins and Nucleic Acids, MacMillan, New York, 1964.
[34] H. Edelhoch, Spectroscopic determination of tryptophan and tyrosine in proteins, Biochemistry 6 (1967) 1948–1954.
[35] S.-Y. Jeon, L.Q. Pi, W.-S. Lee, Comparison of hair shaft damage after UVA and UVB irradiation, J. Cosmet. Sci. 59 (2008) 151–156.
[36] C. Scanavez, I. Joekes, H. Zahn, Extractable substances from human hair: a discussion about the origin of the holes, Colloids Surf. B: Biointerfaces 39 (2004) 39–43.
[37] R.D. Lillie, R. Bangle, E.R. Fisher, Metachromatic basophilia of keratin after oxidation-cleavage of disulfide bond, J. Histochem. Cytochem. 2 (1954) 95–102.
[38] E. Serebryany, J.A. King, The βγ-crystallins: native state stability and pathways to aggregation, Prog. Biophys. Mol. Biol. 115 (2014) 32–41.